

## Fragile-to-strong crossover and polyamorphism in liquid silica: changes in liquid structure

IVAN SAIKA-VOIVOD<sup>†‡||</sup>, FRANCESCO SCIORTINO<sup>†</sup> and PETER H. POOLE<sup>‡§</sup>

<sup>†</sup> Dipartimento di Fisica and Istituto Nazionale per la Fisica della Materia, Università di Roma La Sapienza, Piazzale Aldo Moro 2, I-00185 Roma, Italy

<sup>‡</sup> Department of Applied Mathematics, University of Western Ontario, London, Ontario N6A 5B7, Canada

<sup>§</sup> Department of Physics, St Francis Xavier University, Antigonish, Nova Scotia B2G 2W5, Canada

### ABSTRACT

Previous numerical investigations of model silica have shown evidence favouring liquid–liquid phase separation in the deeply supercooled liquid. This thermodynamic instability is argued to be responsible for the polyamorphic behaviour in the glass. In these previous investigations, a method for discerning local density was developed by writing the radial distribution function as a sum of contributions from neighbours of a given atom, sorted in order of their distance from the given atom. Quite separately, along isochores of densities comparable with that of silica at ambient pressure, simulations have also shown that the Arrhenius dependence of diffusivity on temperature  $T$  so characteristic of liquid silica breaks down at higher temperatures. Indeed, evidence indicates that silica approaches Arrhenius (strong) behaviour upon cooling from higher temperatures where it exhibits super-Arrhenius (fragile) behaviour. We now revisit this fragile-to-strong crossover using the technique of discerning density differences developed in the polyamorphism study. We show that the technique is useful in illustrating the structural change taking place through the crossover. We also see that the structures present in the high-temperature liquid reappear upon increasing density, supporting the observation that fragility increases upon compression of the liquid. Furthermore, we see that these same structures are typical of those which presage the liquid–liquid phase separation at lower temperatures.

### § 1. INTRODUCTION

#### 1.1. *Liquid–liquid phase separation*

Liquid–liquid separation is the extreme form of polyamorphism, a phenomenon described by the existence of more than one amorphous condensed ‘phase’ of a material. A glassy material may undergo a continuous but rapid change in density in response to increasing pressure. This is a subglass transition version of the liquid–liquid transition, where the change in density is a discontinuous function of pressure. Indeed the behaviour of the glass and the liquid may stem from the same underlying

---

|| Author for correspondence. Email: [ivan@systar.phys.uniroma1.it](mailto:ivan@systar.phys.uniroma1.it).

thermodynamics, with the continuous nature of glassy polyamorphism arising from the very slow dynamics of the glass. A general discussion on liquid–liquid phase transitions has been given in Poole *et al.* (1997). Liquid–liquid separation in one-component systems has been shown in computer simulations for water (Poole *et al.* 1992), and recently for more generic systems (Franzese *et al.* 2001).

In our previous work we showed evidence in computer simulations for liquid–liquid phase separation in models of silica (Saika-Voivod *et al.* 2001b). In that work, we used an extrapolation of the potential energy  $U$  to map out the equation of state (EOS) for the liquid at temperatures lower than those at which we could equilibrate the liquid. The extrapolation was based on the functional form  $U(T) = a + bT^{3/5}$  predicted for simple liquids (Rosenfeld and Tarazona 1998). The data for two models of silica, those given by van Beest, Kramer and van Santen (BKS) (1990) and Woodcock, Angell and Cheeseman (WAC) (1976), fit the predicted functional form well and the resulting extrapolated EOS showed a region in the volume–temperature plane where the liquid becomes thermodynamically unstable, separating into two liquids of different densities. The state points used and the resulting liquid–liquid spinodal line for BKS silica are shown in figure 1.

From more recent simulations, we know that the extrapolation used for the potential energy breaks down, at least for BKS silica, at temperatures lower than shown in figure 1. Therefore, the location of the spinodal line shown in figure 1

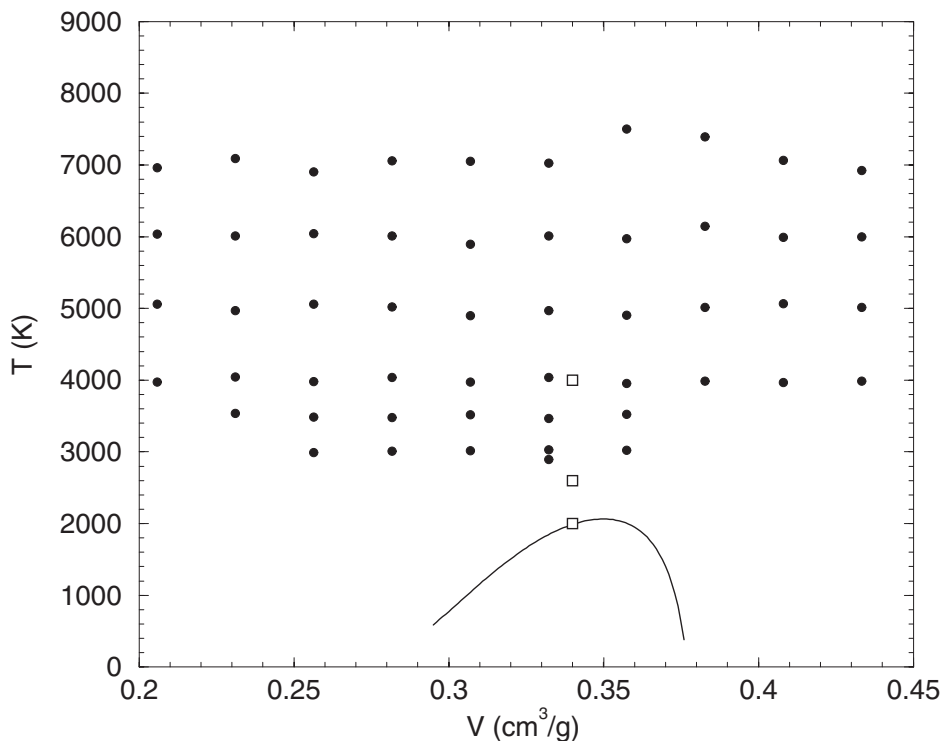


Figure 1. State points used to study the liquid–liquid transition in BKS silica: (●), equilibrated state points with 1332 particles; (□), state points along an isochore chosen to probe the unstable region. Only the highest-temperature point along this isochore is equilibrated fully. The liquid–liquid spinodal is also shown (—).

is not precise. Nonetheless, as direct evidence has shown, liquid–liquid separation does occur within the region, at least along the isochore used to probe the region (open squares in figure 1).

We now discuss the method we used to discern local density differences within the small simulation box. We begin with the pair (radial) distribution function  $g(r)$  defined so that  $4\pi r^2 g(r) dr$  gives the probability of finding a particle between  $r$  and  $r + dr$  of a given particle relative to a randomly distributed system. We then write the pair distribution function as a sum of neighbour contributions, that is

$$g(r) = \sum_i g_i(r). \quad (1)$$

For example,  $g_1(r)$  gives the probability density of finding the closest particle to a given particle at a distance  $r$ , while  $g_2(r)$  gives the probability of finding the second closest particle, and so on. This is related to, but distinct from, neighbour shells. For example, in the case where a Si atom is surrounded by four O atoms, the first-neighbour shell is given by the sum  $g_1(r) + g_2(r) + g_3(r) + g_4(r)$ . In simpler terms, measuring  $g_i(r)$  answers the question: ‘Given a particle, where is the  $i$ th-closest particle located?’

Furthermore, we restrict our discussion to Si atoms. For the following discussion,  $g_i(r)$  indicates the location of the  $i$ th-nearest Si neighbour of a given Si atom. We expect that in a homogeneous liquid each  $g_i(r)$  is a unimodal distribution with a well-defined mean and variance, whereas for a phase-separated liquid, where we find coexistence of two liquids each with a different density, we might expect bimodal distributions to emerge in at least one of the  $g_i(r)$  distributions. In other words, the local structure of the denser liquid must be more compact, and hence atoms will be closer together. On some length scale, or on the scale of some neighbour distance, the distributions of the two liquids may be sufficiently different to discern an overall bimodality in the resulting  $g_i(r)$ .

The results of using individual Si–Si neighbour contributions to  $g(r)$  are shown in figure 2, where results for both the BKS and the WAC potentials are shown. The figure shows  $g_5(r)$  for three temperatures along the isochore chosen to probe the suspected region of instability. At high temperatures the distribution is indeed unimodal. As the temperature is reduced, a shoulder develops until finally at the lowest temperature the distribution becomes bimodal. The bimodal structure allows us to assign a threshold radius  $r^*$  to be used in labelling Si atoms as belonging to either the higher- or the lower-density phase. For example, a Si atom with its fifth-nearest neighbour lying closer than  $r^*$  is considered to be of the denser fluid and is represented by a dark sphere in figure 3. We note that, at the lowest temperature, equilibrium is not obtained; that is, the potential energy of the system continues to decrease after long simulation times, presumably as a result of the continued coarsening of the liquid domains. Figure 3 shows that Si atoms belonging to different density environments are indeed spatially correlated, a necessary condition for phase separation.

### 1.2. Fragile-to-strong crossover

Now we turn our attention to the study of the fragile-to-strong crossover in liquid silica. Silica is the archetypal ‘strong’ liquid (Richet 1984, Angell 1991), exhibiting an Arrhenius dependence of relaxation parameters, such as the diffusivity  $D$ ,

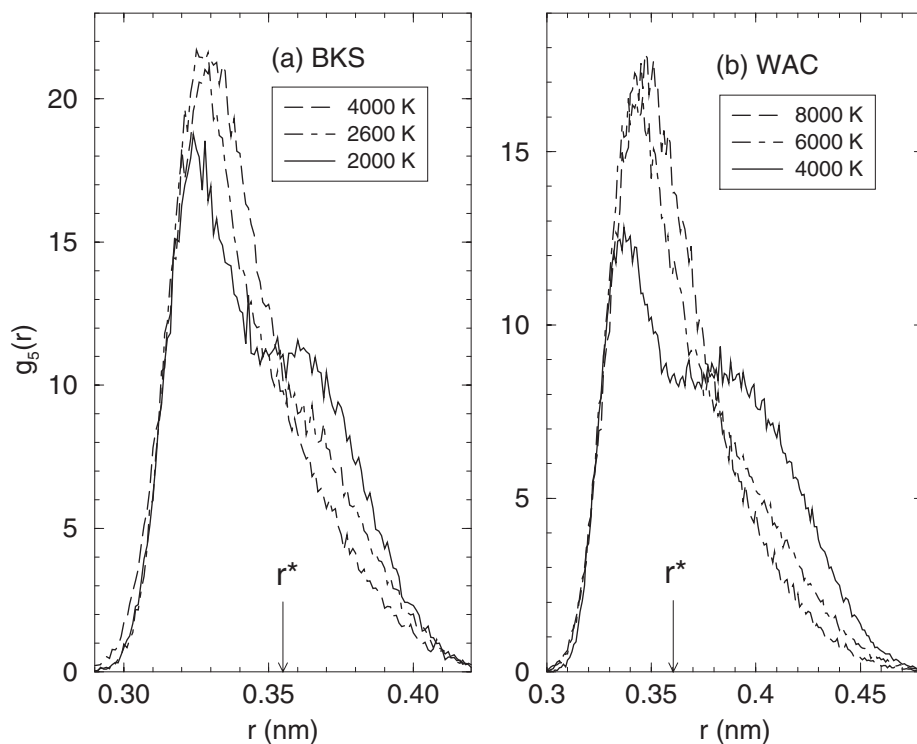


Figure 2. The distribution of fifth Si-Si neighbours  $g_5(r)$ . Lowering the temperature along a nearly critical isochore produces a bimodal distribution in the distribution in both the BKS and the WAC silica potentials. The bimodality shows that there are two distinct density environments present in the simulation cell.

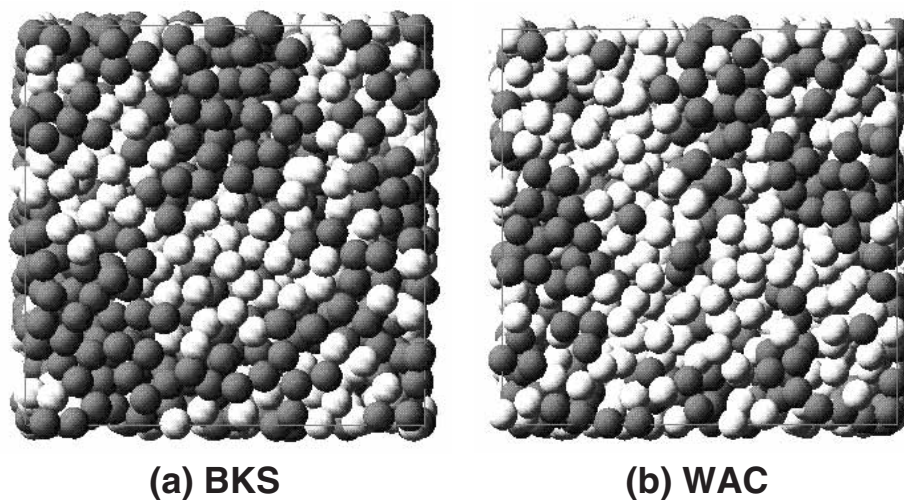


Figure 3. Evidence of liquid-liquid separation. After using the threshold radius to label Si atoms as belonging to either the low- or high-density liquid, a snapshot configuration shows the presence of strong spatial correlation between Si atoms of similar densities.

on the temperature  $T$ . Indeed silica maintains an Arrhenius behaviour on heating from the glass transition temperature over a large temperature range.

Molecular dynamics computer simulations of BKS silica (Horbach and Kob 1999) have shown, however, that at higher temperatures the Arrhenius behaviour is lost and the liquid behaves as a typical ‘fragile’ liquid. Thus, liquid silica crosses over to the strong regime from a fragile regime upon cooling. In our previous work (Saika-Voivod *et al.* 2001a), we showed that this crossover is intimately linked to the potential energy landscape of the liquid. To do this we employed the inherent structure (IS) formalism (Stillinger and Weber 1984), where each configuration of atoms is mapped to a local potential energy minimum through a path of steepest descent. More abstractly, one can think of the potential energy as a function of the  $3N$  coordinates of the system (three degrees of freedom for each of  $N$  particles). This function is a surface in a  $(3N + 1)$ -dimensional space, and is pitted with local minima, with crystal structures representing deep minima. The vast majority of minima, however, are amorphous configurations. In the IS formalism we can write the equilibrium liquid free energy as (Sciortino *et al.* 1999, La Nave *et al.* 2003)

$$F_{\text{liq}}(e_{\text{IS}}, T) = e_{\text{IS}}(T) - TS_{\text{c}}(e_{\text{IS}}) + f_{\text{vib}}(e_{\text{IS}}, T), \quad (2)$$

where  $e_{\text{IS}}(T)$  is the average value of the local energy minima explored by the liquid at temperature  $T$ ,  $S_{\text{c}}(e_{\text{IS}})$  is the configurational entropy and  $f_{\text{vib}}(e_{\text{IS}}, T)$  is the vibrational free energy of a single basin. By a basin we mean the collection of configurations connected via a steepest-descent path to a local minimum, where the potential energy is  $e_{\text{IS}}$ . The configurational entropy  $S_{\text{c}}$  counts the number of basins. More precisely, if  $\Omega(e_{\text{IS}})\delta e_{\text{IS}}$  is the number of minima with energy between  $e_{\text{IS}}$  and  $e_{\text{IS}} + \delta e_{\text{IS}}$ , then  $S_{\text{c}}(e_{\text{IS}}) = k_{\text{B}} \ln [\Omega(e_{\text{IS}})]$ .

With the assumption that basin vibrational properties do not vary significantly with  $e_{\text{IS}}$ , an assumption justified by what we observed in the case of BKS silica, we can minimize the free energy with respect to  $e_{\text{IS}}$  and obtain

$$S_{\text{c}}(T) = S_{\text{c}}(T_0) + \int_{T_0}^T \frac{1}{T'} \frac{\partial e_{\text{IS}}}{\partial T'} dT'. \quad (3)$$

The other key ingredient in our analysis of the fragile-to-strong transition is the Adam–Gibbs (1965) relationship, relating the diffusivity  $D$  to  $S_{\text{c}}$ :

$$D(T) = D_0 \exp\left(-\frac{A}{TS_{\text{c}}(T)}\right), \quad (4)$$

where  $D_0$  and  $A$  are constants with respect to temperature  $T$ . In our previous work, we showed that this relation holds for BKS silica. We see that, if  $S_{\text{c}}(T)$  is constant with temperature, then we recover Arrhenius behaviour

$$D(T) = D_0 \exp\left(-\frac{B}{T}\right). \quad (5)$$

We note that Arrhenius behaviour can also be achieved if  $S_{\text{c}}(T) = C/(T^* - T)$ . At present, we disregard this case, although it may prove to be an interesting avenue to explore in the future.

As is evident from equation (3) the temperature dependence of  $S_{\text{c}}$  arises from the temperature dependence of  $e_{\text{IS}}$ . Furthermore, if  $e_{\text{IS}}$  becomes constant, then  $S_{\text{c}}$  will also reach a constant value and Arrhenius behaviour will be recovered.

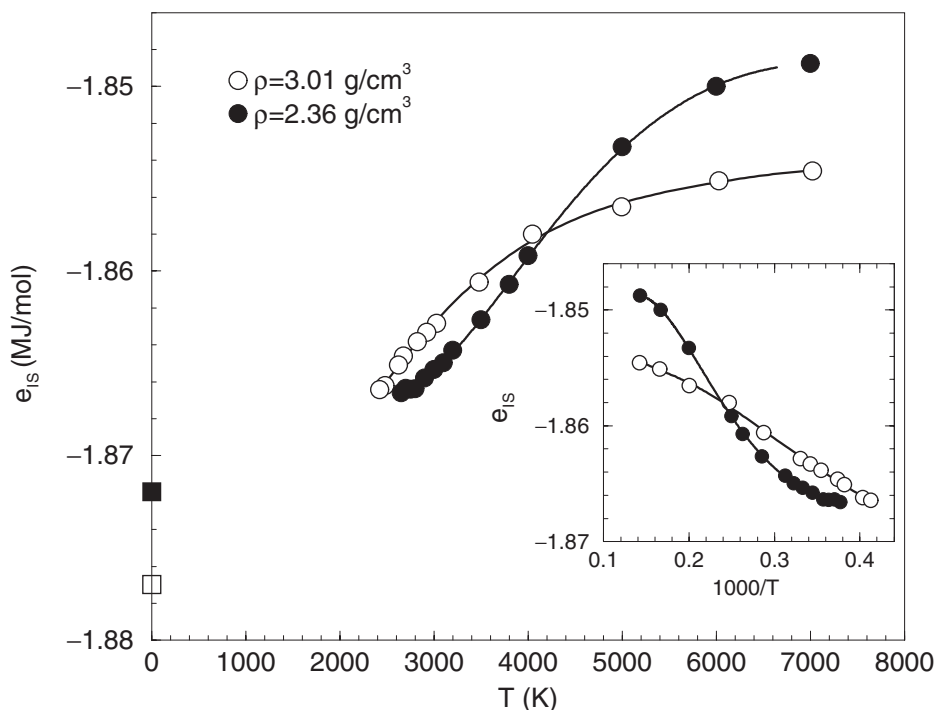


Figure 4. IS energy as a function of temperature  $T$  for two isochores. The higher-density isochore, where no fragile-to-strong transition is observed on cooling, follows the  $1/T$  dependence typical of fragile liquids (inset). The lower density, which undergoes the fragile-to-strong transition, exhibits an inflection. The full (open) square shows the crystal energy corresponding to the density labelled by full (open) circles.

In figure 4 we show  $e_{IS}(T)$  for two densities: one high and one low. Both isochores show a negative curvature at high temperatures, although only the higher density exhibits the  $1/T$  behaviour characteristic of fragile liquids (inset). We note that the  $1/T$  behaviour arises from a Gaussian distribution of IS energies (Sastry 2001). Hence, BKS silica, at densities where it shows strong behaviour, does not possess a Gaussian distribution of IS energies. In the case of the low-density isochore, where the strong-to-fragile crossover is observed, the curve indeed inflects near 4000 K and exhibits positive curvature at low temperatures. This inflection is necessary if the curve is to approach a constant value. Indeed it is a necessary condition for the dynamic crossover. We also plot in the same figure estimates of the underlying crystal ground states as plausible lower bounds on  $e_{IS}$ . The crystal energy estimates are consistent with the inflection seen in the lower-density isochore. For the higher density, the lower bound would only necessitate an inflection at much lower temperatures.

Thus we see that the behaviour of  $e_{IS}$  drives the dynamic transition through the  $S_c$  and the Adam–Gibbs relationship. What we now explore is the structural change that occurs as the liquid undergoes this transition, and whether there is any evidence for a structural connection between the dynamic transition and polyamorphism.

The evaluation of the configurational entropy, as well as the use of the Adam–Gibbs relation briefly described above, is similar to work done previously in simulations of water (Scala *et al.* 2000, Starr *et al.* 2001) as well as for orthoterphenyl

(Mossa *et al.* 2002). The Adam–Gibbs relationship has also recently been used to describe the dynamics of chemical vitrification (Corezzi *et al.* 2002).

## §2. STRUCTURAL CHANGE IN THE EQUILIBRIUM LIQUID

We now apply the technique used to determine local density differences in the case of polyamorphism, namely the expansion of  $g(r)$  in terms of neighbours, to the problem of identifying structural changes in the liquid across the fragile-to-strong transition. To this end we plot  $g_i(r)$  in figure 5 for  $i = 1, \dots, 8$ , for three equilibrium state points: at a low density above the fragile-to-strong crossover ( $T = 5000$  K), at a low density below the fragile-to-strong crossover ( $T = 2900$  K), and at  $T = 2900$  K for a higher density where the liquid retains its fragile character over all studied temperatures. We stress that the  $g_i$  values are for Si–Si distances.

For all the state points shown in figure 5, the first four Si neighbours of a given Si are all well behaved and lie in the first-neighbour shell. The differences between the structures of the state points lies primarily in the location of the fifth neighbour. At high temperatures and low densities (figure 5 (a)), the fifth-neighbour distribution

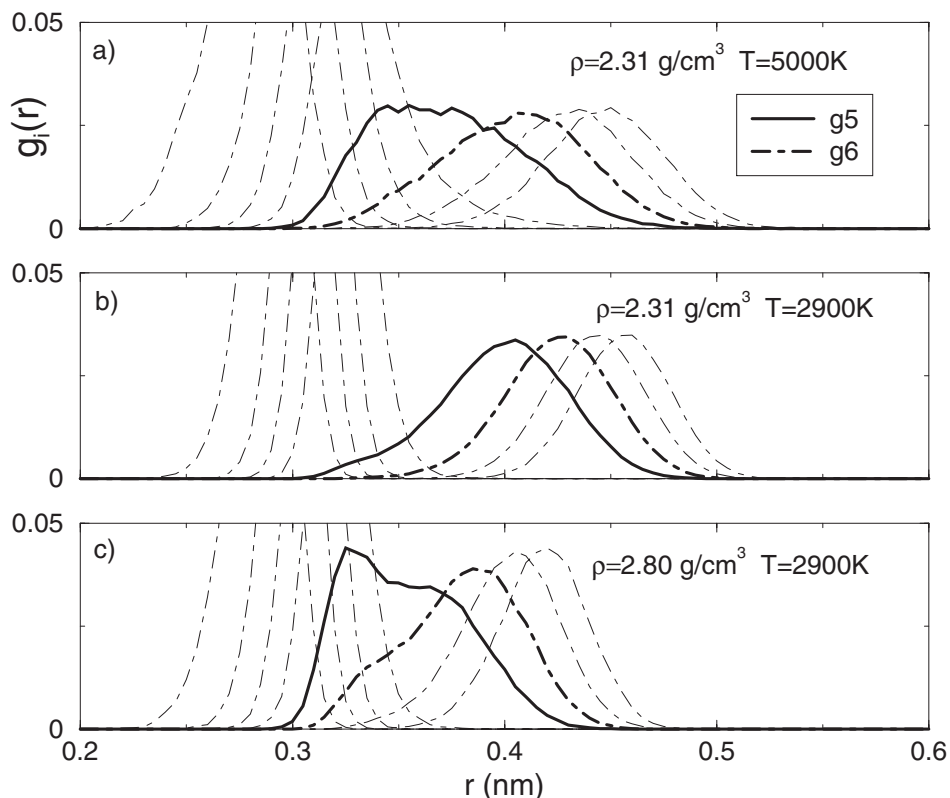


Figure 5. Structural changes with changing temperature  $T$  and density  $\rho$ : (a)  $g_i(r)$  for a low-density isochore at a temperature above the fragile-to-strong crossover (above the inflection in  $e_{\text{IS}}(T)$ ); (b) the same quantities after cooling below the inflection; that is where the liquid is tending to a strong liquid; (c) a higher-density state point at the same low temperature. All state points are in equilibrium. The curves for  $g_5$  and  $g_6$  highlight structural changes.

is broad, with a significant portion of the distribution contributing to the first-neighbour shell.

Here we pause to think what results should arise from a similar analysis of a good tetrahedral network. In silica, the tetrahedra each have a Si atom in the centre, with an O atom at each of the four corners. For a corner-sharing network, therefore, there are four tetrahedra surrounding any given tetrahedron. Thus, we expect four Si atoms in the first Si–Si neighbour shell for a liquid in which a good network has formed.

We see from figure 5 that, at high temperatures, the fifth Si neighbour ‘crowds’ the first-neighbour shell and prevents the formation of a good network. As the temperature is lowered well below the inflection point along the same isochore, we see a large reduction in the number of fifth (and sixth) neighbours in the first-neighbour shell (figure 5(b)). We conclude that the quality of the network has improved significantly. If strong behaviour in silica is associated with a ‘tear and repair’ of a well-formed network, then we have a consistent picture developing, in which the fragile-to-strong dynamic crossover is accompanied by the continuing formation of a good network.

If we now turn to figure 5(c), we see that, at a higher density, where the liquid is fragile for all of the temperatures studied, a portion of the fifth and sixth neighbours again crowds the first-neighbour shell. Thus, in an instantaneous snapshot of the liquid, many Si atoms are not part of well-formed networks. These ‘structural impurities’ serve to disrupt the network and hence are responsible for the fragile behaviour, perhaps analogous to the way that chemical additives increase the fragility in silica.

Figure 5(c) also shows a bimodal distribution  $g_5(r)$  in an equilibrium liquid that is not phase separated. This is intriguing. The result indicates that there are two distinct density or structural environments present in the liquid, although they are mixed. The shapes of  $g_5(r)$  and  $g_6(r)$  suggest that one environment has four Si atoms in the first-neighbour shell, while the other has five or six. If the liquid phase separates at lower temperatures, then we shall have coexistence of a liquid with a good network (presumably a strong liquid) and a liquid with a poor network (fragile). This idea supports the hypothesis that the fragile-to-strong dynamic crossover is the extension into the equilibrium liquid of an underlying liquid–liquid phase transition.

In general,  $g_i(r)$  may be useful in describing the connection between liquid structure and other properties, for example diffusivity, as the density and temperature change. Recent work on model silica (Shell *et al.* 2002) examined the connection between structural order and silica’s density and diffusivity anomalies. Perhaps the neighbour distribution analysis presented here may also provide some insight into questions pertaining to structural change.

### §3. CONCLUSIONS

The decomposition of  $g(r)$  into contributions from successive neighbours is a useful tool in examining liquid structure in computer simulations. We used this technique to discern liquid–liquid phase separation in supercooled silica and now we use it to see structural change that accompanies the fragile-to-strong dynamic transition in low-density liquid silica. We associate the structural change with the formation of a more ordered tetrahedral network.

As the density is increased, we see with this technique that disorder is reintroduced into the network. We also see bimodal neighbour distributions in the



equilibrium liquid where there is no phase separation, indicating the presence of separate liquid structures. We conjecture that, upon lowering the temperature, these structures no longer mix but rather phase separate. This scenario is consistent with the hypothesis that there is a strong connection between the fragile-to-strong crossover and a low-temperature liquid-liquid critical point.

#### ACKNOWLEDGEMENTS

P.H.P. and I.S.-V. wish to thank Natural Sciences and Engineering Research Council (Canada) for funding. F.S. wishes to thank Ministero dell'Istruzione, dell'Università e della Ricerca (MIUR), Progetti di Ricerca di rilevante Interesse Nazionale (PRIN) COFIN and Fondo per gli Investimenti della Ricerca di Base (FIRB) for support.

#### REFERENCES

- ADAM, G., and GIBBS, J. H., 1965, *J. chem. Phys.*, **43**, 139.  
ANGELL, C. A., 1991, *J. non-crystalline Solids*, **131**, 13.  
COREZZI, S., FIORETTO, D., and ROLLA, P., 2002, *Nature*, **420**, 653.  
FRANZESE, G., MALESCIO, G., SKIBINSKY, A., BULDYREV, S. V., and STANLEY, H. E., 2001, *Nature*, **409**, 692.  
HORBACH, J., and KOB, W., 1999, *Phys. Rev. B*, **60**, 3169.  
LA NAVE, E., SCIORTINO, F., TARTAGLIA, P., DE MICHELE, C., and MOSSA, S., 2003, *J. Phys.: condens. Mater.*, **15**, S1085.  
MOSSA, S., LA NAVE, E., STANLEY, H. E., DONATI, C., SCIORTINO, F., and TARTAGLIA, P., 2002, *Phys. Rev. E*, **65**, 041 205.  
POOLE, P. H., GRANDE, T., ANGELL, C. A., and McMILLAN, P. F., 1997, *Science*, **275**, 322.  
POOLE, P. H., SCIORTINO, F., ESSMANN, U., and STANLEY, H. E., 1992, *Nature*, **360**, 324.  
RICHET, P., 1984, *Geochim. Cosmochim. Acta*, **48**, 471.  
ROSENFELD, Y., and TARAZONA, P., 1998, *Molec. Phys.*, **95**, 141.  
SAIKA-VOIVOD, I., POOLE, P. H., and SCIORTINO, F., 2001a, *Nature*, **412**, 514.  
SAIKA-VOIVOD, I., SCIORTINO, F., and POOLE, P. H., 2001b, *Phys. Rev. E*, **63**, 011 202.  
SASTRY, S., 2001, *Nature*, **409**, 164.  
SCALA, A., STARR, F. W., LA NAVE, E., SCIORTINO, F., and STANLEY, H. E., 2000, *Nature*, **406**, 166.  
SCIORTINO, F., KOB, W., and TARTAGLIA, P., 1999, *Phys. Rev. Lett.*, **83**, 3214.  
SHELL, M. S., DEBENEDETTI, P. G., and PANAGIOTOPOULOS, A. Z., 2002, *Phys. Rev. E*, **66**, 011 202.  
STARR, F. W., SASTRY, S., LA NAVE, E., SCALA, A., STANLEY, H. E., and SCIORTINO, F., 2001, *Phys. Rev. E*, **63**, 041 201.  
STILLINGER, F. H., and WEBER, T. A., 1984, *Science*, **225**, 983.  
VAN BEEST, B. W. H., KRAMER, G. J., and VAN SANTEN, R. A., 1990, *Phys. Rev. Lett.*, **64**, 1955.  
WOODCOCK, L. V., ANGELL, C. A., and CHEESEMAN, P. A., 1976, *J. chem. Phys.*, **65**, 1565.